International Journal of Engineering & Technology, 7 (3.18) (2018) 16-20

International Journal of Engineering & Technology

Website: www.sciencepubco.com/index.php/IJET

Technical paper

Morphological and Otsu's Thresholding-Based Retinal Blood Vessel Segmentation for Detection of Retinopathy

Kuryati Kipli[1]*, Cripen Jiris[1], Siti Kudnie Sahari[1], Rohan Sapawi[1], Nazreen Junaidi[1], Marini Sawawi[2], Kismet Hong Ping[1], Tengku Mohd Afendi Zulcaffle[1]

[1]Department of Electrical and Electronic Engineering, Faculty of Engineering, Universiti Malaysia Sarawak
[2]Department of Mechanical and Manufacturing Engineering, Faculty of Engineering, Universiti Malaysia Sarawak
**Corresponding author E-mail: kkuryati@unimas.my*

Abstract

Retinal blood vessel segmentation is crucial as it is the earliest process in measuring various indicators of retinopathy sign such as arterial-venous nicking, and focal arteriolar and generalized arteriolar narrowing. The segmentation can be clinically used if its accuracy is close to 100%. In this study, a new method of segmentation is developed for extraction of retinal blood vessel. In this paper, we present a new automated method to extract blood vessels in retinal fundus images. The proposed method comprises of two main parts and a few subcomponents which include pre-processing and segmentation. The main focus for the segmentation part is two morphological reconstructions which are the morphological reconstructions followed by the morphological top-hat transform. Then the technique to classify the vessel pixels and background pixels is Otsu's Thresholding. The image database used in this study is the High Resolution Fundus Image Database (HRFID). The developed segmentation method accuracies are 95.17%, 92.06% and 94.71% when tested on dataset of healthy, diabetic retinopathy (DR) and glaucoma patients respectively. Overall, the performance of the proposed method is comparable with existing methods with overall accuracies were more than 90 % for all three different categories: healthy, DR and glaucoma.

Keywords: *Detection; Morphological; Retinal blood vessels; Retinopathy; Segmentation; Thresholding.*

1. Introduction

Retinal blood vessel segmentation is crucial image processing step before performing feature extraction in retinal analysis. In retinal analysis, segmented blood vessel is useful for microvasculature analysis, vascular geometry extraction, measurement of various parameter such as artery and vein ratio. Retinal blood vessel segmentation also enable detection of haemorrhages, microaneurysms, irregularities in the route of blood vessels and neovascularization [1-5]. The accuracy of retinal blood vessel segmentation is important to ensure accurate extraction and measurement of features for detection/diagnosis of retinal related diseases, including stroke [6], hypertensive retinopathy (HR) [7], diabetic retinopathy [8], and retinopathy of prematurity [9]. Manual segmentation of the blood vessel is time consuming and prone to human error, thus not practical when number of images is large and the vessel structures are complicated [10, 11]. As a result, an automated blood vessels segmentation algorithm is desired.

Several automated methods have been developed to get accurate blood vessel segmentation [8]. The drawback of existing techniques is that they generally output poor segmentation results when applied on unhealthy retinal images that have the presence of lesions [11]. They also need more computational power when the size of an image increases, thus a simple yet fast method is required for real time processing.

In this paper, we present a new automated method to extract blood vessels in retinal fundus images. The main contributions of this study include: i) proposed new methodology for retinal blood vessel segmentation, ii) apply the proposed method of retinal blood vessel segmentation on the retinal fundus image of healthy and unhealthy subjects and iii) evaluate the performance of the proposed method by analyzing performance metrics such as accuracy, specificity and sensitivity and compare against existing techniques.

2. Related Work

The segmentation method can be divided into supervised and unsupervised method. In a supervised method, [11] used neural network to develop a pixel tracking based approaches or vectorial tracking or tracing to segment the retina blood vessel branches or structure. In this method, the retinal blood vessel is initially tracked by the detection of initial vessel seed points and then only the rest of the vessel pixels tracked by measuring the continuity of blood vessel characteristics. [2] used two neural network trainers for hierarchical retinal blood vessel segmentation process. The two trainers are known as convolutional neural network (CNN) and random forest (RF) classifier. CNN is a trainable hierarchical feature extractor and with the help of RF as a trainable classifier.

The unsupervised method or known as pixel processing based method process every pixel in the image and apply multiple operations on each pixel [10, 11]. An example of this technique is by [12]. The technique was first done the filtering enhancement of the retinal blood vessel by using multiple scales filtering technique based on the eigenvalue analysis of the Hessian matrix. After the contrast between vessels and other tissues is vastly improved then only an iterative thresholding method is applied on the retinal

Copyright © 2018 Authors. This is an open access article distributed under the Creative Commons Attribution License, which permits unrestricted use, distribution, and reproduction in any medium, provided the original work is properly cited.

images. The thresholding method used in this problem is named Otsu's Thresholding [12].

Generally, a conventional retinal blood vessel segmentation process is as shown in Figure 1 in form of a flow chart [17]. It consists of conversion of original image to grey-scale image, image enhancement, vessel segmentation and extraction. Grey-scale image is a data matrix whose values represent intensities within some range. In single colour channel the channel's intensity is manipulated as the grey-scale intensity. Image enhancement is a technique to improve the visual appearance of an image or to convert the image to a better form for human or computer analysis. The vessel segmentation and vessel extraction are very important in order to recognize the retinal blood vessels branches or structure.

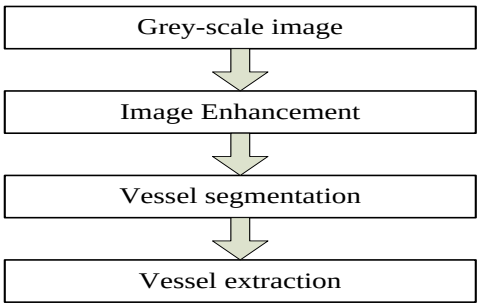


Fig. 1: Conventional retinal blood vessel segmentation process [13]

3. Materials and Methods

3.1. Software

The software used in this research is MATLAB (R2011a). The simulation was run on the personal computer with operating system Windows 7 Ultimate, microprocessor name is Pentium (R) Dual-Core CPU, 4 GB random access memory, and 64-bit operating system.

3.2. Image Database

In this study, fundus images of retinal were used as it captured the blood vessel of the retina clearly. Retinal images dataset named High Resolution Fundus Image Database (HRFID) [14] were employed. HRFID is available publicly [12]. This database developed by two European institutions which are Brno University of Technology, Faculty of Electrical Engineering and Communication, Department of Biomedical Engineering, Brno, Czech Republic, and Pattern Recognition Lab at the University of Erlangen – Nuremberg, Germany [14]. The retinal images were captured by fundus camera CANON CF–60 UVi equipped with CANON EOS–20D digital camera with a 60-degree field of view. The images were true colour image or in RGB colour image with size of 3504 × 2336 pixels. All images are stored in JPEG format with low compression rates.

The manual segmentation of the retinal blood vessel for this database was also provided. Segmentation were performed by three experts working in the field of retinal image analysis. These experts were trained by experienced ophthalmologists from the ophthalmology clinic where the images were taken and they were asked to label all pixels belonging only to retinal vessels [14]. An image editing software ADOBE Photoshop CS4 image editor was used for manual labelling.

This database image contains 15 retinal images of healthy patients, 15 retinal images of patients having diabetic retinopathy disease, and 15 retinal images of patients experiencing glaucoma disease.

3.4. The Proposed Method

The proposed method is shown in Figure 2. It consists of two main parts which are pre-processing and segmentation. For pre-processing part, it comprises of two main components while segmentation comprises of four main components. Further detail on these components will be explained in subsequent sections.

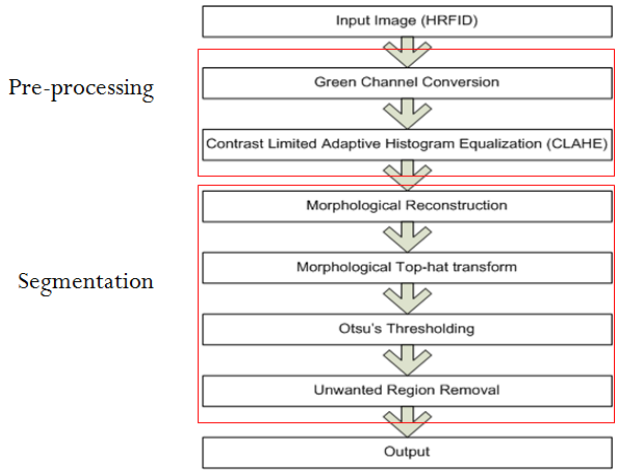


Fig. 2: Proposed methodology

3.4.1. Pre-Processing

The processes begin by conversion of the input image from the colour image format to the grey-scale image format. This was performed using green channel. Then, the green channel is inverted using the inverted function. The next step is enhancing the grey-scale image using Contrast Limited Adaptive Histogram Equalization (CLAHE) [17] enhancement to reveal the contrast of the vasculature. For CLAHE the distribution parameter used is exponential while the clipLimit parameter value is 0.03. The green channel is used due to it characteristics that revealing retinal blood vessels [1, 2, 15, 16] more than any other two channels. The green channel image is inverted to make the blood vessel become brighter compared to the background.

3.4.2. Segmentation

The morphology processing technique is chosen due to the nature of the process suitable for extracting the biological feature in an image. The two process used is to ensure the vasculature extracted before the image is threshold. The morphology reconstruction used is the complementary of opening-by-reconstruction and closing-by-reconstruction.

The opening-by-reconstruction equation is as shown in Equation 1 which defined as the opening by reconstruction of size n of an image f is equal to the reconstruction by dilation of f from the erosion of size n of f. Equation 2 is closing-by-reconstruction and its definition is closing by reconstruction of size n of an image f is equal to the reconstruction by erosion of f from the dilation of size n of f. The structuring parameter used is 'square' and its size is 10 for the opening-by-reconstruction part to complete the morphological reconstruction processing. The morphological top-hat transform is the difference between an image and its output results after processed using opening with structuring element as shown in Equation 3. In the process of the image under this morphology transform the image intensity is also adjusted. The structuring parameter used is 'octagon' and its size is 45 for succeeding the morphological top-hat transform processing.

$$O_R^{(n)}(f) = R_f^D[(f \ominus nb)] \quad (1)$$

$$C_R^{(n)}(f) = R_f^E[(f \oplus nb)] \quad (2)$$

$$f_{Top-hat} = f - (f \ominus b) \quad (3)$$

Otsu is an analysis using the threshold that minimizes the within-class variance of the thresholded black and white [17]. Unwanted region removal is act like a filter that filters small region of noise to improve the accuracy of the proposed method.

The proposed method mainly used the analysis of histogram processing for adjustment of parameter. The bimodal graph shape of histogram of the image must be obtained so that Otsu's Thresholding can be effectively implemented. Although the image processing techniques employed in this proposed method is similar to some reported work, the main difference is the sequence of the processing and a few main components different. For example, [17] used Matrix and Eigenvalue approach before thresholded using local Otsu's Thresholding.

3.5. Performance Metrics

To evaluate the performance of the method used the following metrics which are Sensitivity (Se), Specificity (Sp), Positive Predictive Value (PPV), Negative Predictive Value (NPV), and Accuracy (Acc) [25].

$$Se = \frac{TP}{TP + FN} \quad (4)$$

$$Sp = \frac{TN}{TN + FP} \quad (5)$$

$$PPV = \frac{TP}{TP + FP} \quad (6)$$

$$NPV = \frac{TN}{TN + FN} \quad (7)$$

$$Acc = \frac{TP + TN}{TP + FN + TN + FP} \quad (8)$$

Where:
Se = the ratio of well-classified vessel, Sp = ratio of non-vessel pixels, PPV =ratio of correctly classified vessel pixels, NPV= ratio of correctly classified non-vessel pixels, Accuracy= proportion of true result, TP= true positive, FP=false positive, TN=true negative, FN=false negative

4. Results and Discussion

This section presents the performance results of the proposed methods. First, the output images at each step of the proposed method are shown. Second, the accuracy, specificity, and negative predictive value of the proposed method when implemented on three different categories: healthy, DR and glaucoma are presented. Lastly, the performance of this proposed method are compared three works from [14], [18] and [19]. [18] combined the RF, and feature extractor such as stroke width transform and Weber's local descriptors on HRFID. [19] performed a novel inpainting filter which called the neighbourhood estimator is to inpaint exudates to reduced greatly false vessel detection due to exudates which were enhanced during vessel enhancement. For the segmentation a percentile-based thresholding which thresholding the cumulative histogram of the Hessian enhanced image. [14] improved the matched filtering method and classified the vessel using Kittler minimum error thresholding method.

Figure 3 shows the outputs image of each step in the proposed method. Figure 3(a) is the input image, Figure 3(b) is the green channel image, and then the image is through inversion process so that the vessel pixels become white while background pixels become dark or black. Before the output of the image in Figure 3(b)

was obtained, four experimental colour image into grey scale image conversion was tested which were the conversion through the syntax rgb2gray ( ) which is a function in MATLAB to convert colour image into grey scale image, andim(:,:,1), im(:,:,2) and im(:,:,3) which is the manipulation of the red, green, and blue channel of the image respectively. From the experiment, green channel conversion provides a clear retinal blood vessel structure.

Figure 3(c) is the image after CLAHE applied. In CLAHE the syntax:

g = adapthisteq (f, param1, val1, param2, val2, ...)

where, f is the image, param1 used was clipLimit and itsval1 tested were 0.03, 0.06, and 0.09. For param2, the Distribution was chosen and the values of val2 tested were uniform, Rayleigh, and Exponential.

For the segmentation part, Figure 3(d) is the output image of the morphological reconstruction and Figure 3(e) is the result of the morphological top-hat transform. Then the process of segmentation is completed using Otsu's Thresholding as shown in Figure 3(f) and finally Figure 3(g) is the overall process of the proposed method.

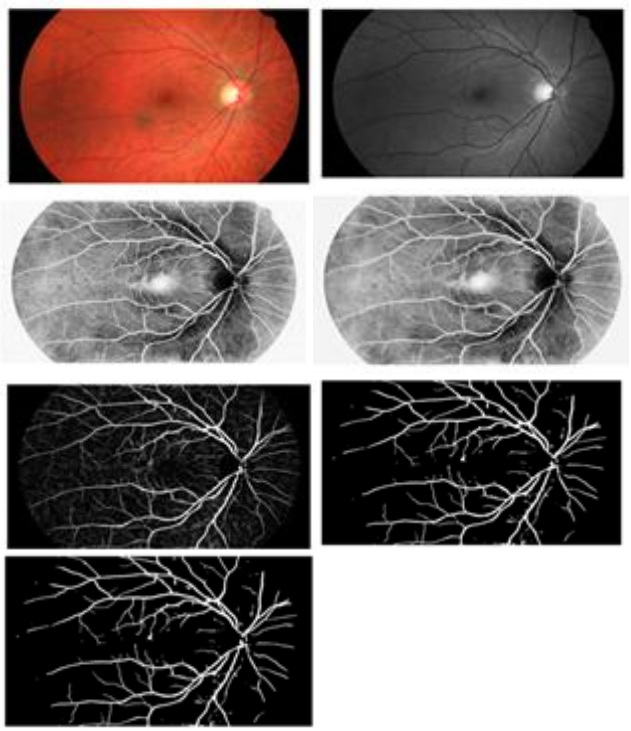


Fig. 3: Outputs image of the proposed method at each steps, (a) input image/original image, (b) green channel image, (c) CLAHE, (d) morphological reconstruction, (e) morphological top-hat transform, (f) Otsu's Thresholding, (g) unwanted region removal.

Table 1, 2 and 3 shows the accuracy, specificity, and negative predictive value of the proposed method in healthy images, DR and glaucoma respectively. In Table 1, the accuracy, specificity, and negative predictive value of the proposed method in healthy images are more consistent as their standard deviations are 0.00734, 0.00651, and 0.00483 respectively. In Table 2, the DR images the most consistent metric is only negative predictive value due to the value of the standard deviation of 0.00624. In glaucoma images the smallest tabulated value of standard deviation in Table 3 is only on the negative predictive value. The value of the standard deviation is 0.00278. For the time taken of the proposed method to process on the HRFID, the healthy images with standard deviation 1.95242 seconds are more consistent than DR and glaucoma images.

Table 1: Performance of accuracy, sensitivity, specificity, positive predictive value, negative predictive value, and time analysis of the healthy retinal images.

Database Files	Acc	Se	Sp	PPV	NPV	Time (s)
01_h	0.9515	0.6613	0.9845	0.8283	0.9624	20.170
02_h	0.9542	0.7674	0.9747	0.7684	0.9745	22.371
03_h	0.9370	0.6398	0.9720	0.7297	0.9581	21.390
04_h	0.9428	0.6776	0.9704	0.7045	0.9666	22.231
05_h	0.9576	0.6753	0.9856	0.8228	0.9684	22.165
06_h	0.9548	0.7353	0.9796	0.8027	0.9704	22.278
07_h	0.9563	0.6725	0.9840	0.8044	0.9685	21.736
08_h	0.9557	0.7210	0.9819	0.8167	0.9693	23.281
09_h	0.9490	0.6746	0.9721	0.6710	0.9726	22.448
10_h	0.9411	0.6878	0.9650	0.6496	0.9704	28.941
11_h	0.9598	0.7381	0.9826	0.8141	0.9733	21.393
12_h	0.9606	0.7742	0.9825	0.8380	0.9738	21.693
13_h	0.9528	0.7176	0.9752	0.7339	0.9732	21.408
14_h	0.9440	0.6900	0.9682	0.6750	0.9703	21.512
15_h	0.9584	0.7287	0.9779	0.7374	0.9770	22.304
Average	0.9517	0.7041	0.9771	0.7598	0.9699	22.355
Standard deviation	0.0073	0.0396	0.0065	0.0639	0.0048	1.952
Maximum	0.9606	0.7742	0.9856	0.8380	0.9770	28.941

*Sensitivity (Se), Specificity (Sp), Positive Predictive Value (PPV), Negative PredictiveValue (NPV), Accuracy (Acc)

Table 2: Performance of accuracy, sensitivity, specificity, positive predictive value, negative predictive value, and time analysis of the diabetic retinopathy retinal images.

Database Files	Acc	Se	Sp	PPV	NPV	Time (s)
01_dr	0.9210	0.8371	0.9255	0.3759	0.9907	18.812
02_dr	0.9284	0.7779	0.9386	0.4632	0.9841	22.707
03_dr	0.8573	0.7743	0.8626	0.2660	0.9835	22.552
04_dr	0.8522	0.7846	0.8562	0.2462	0.9852	29.594
05_dr	0.9540	0.7357	0.9685	0.6076	0.9822	26.018
06_dr	0.9378	0.5824	0.9668	0.5892	0.9659	20.577
07_dr	0.9426	0.7421	0.9595	0.6068	0.9778	22.383
08_dr	0.8942	0.7945	0.9024	0.3983	0.9818	22.252
09_dr	0.9420	0.6676	0.9620	0.5604	0.9755	25.483
10_dr	0.9439	0.6889	0.9683	0.6752	0.9701	24.415
11_dr	0.9476	0.7124	0.9694	0.6828	0.9733	30.593
12_dr	0.9326	0.7430	0.9464	0.5029	0.9806	26.305
13_dr	0.9473	0.7137	0.9645	0.5957	0.9787	21.980
14_dr	0.8868	0.7712	0.8964	0.3809	0.9793	21.215
15_dr	0.9208	0.7601	0.9320	0.4389	0.9823	31.274
Average	0.9206	0.7390	0.9346	0.4927	0.9794	24.411
Standard deviation	0.0328	0.0613	0.0386	0.1392	0.0062	3.750
Maximum	0.9540	0.8371	0.9694	0.6828	0.9907	31.274

*Sensitivity (Se), Specificity (Sp), Positive Predictive Value (PPV), Negative PredictiveValue (NPV), Accuracy (Acc)

Table 3: Performance of accuracy, sensitivity, specificity, positive predictive value, negative predictive value, and time analysis of the glaucoma retinal images.

Database Files	Acc	Se	Sp	PPV	NPV	Time (s)
01_g	0.9488	0.7710	0.9616	0.5900	0.9832	18.693
02_g	0.9427	0.7547	0.9578	0.5899	0.9798	26.573
03_g	0.9581	0.7168	0.9728	0.6180	0.9825	29.238
04_g	0.9543	0.7357	0.9693	0.6224	0.9816	25.859
05_g	0.9591	0.7213	0.9757	0.6747	0.9804	29.320
06_g	0.9539	0.7170	0.9713	0.6470	0.9791	31.519
07_g	0.9496	0.7099	0.9663	0.5947	0.9795	26.229
08_g	0.9255	0.8008	0.9346	0.4712	0.9847	26.007
09_g	0.9534	0.6968	0.9716	0.6350	0.9784	25.615
10_g	0.9551	0.7448	0.9699	0.6345	0.9819	23.592
11_g	0.9532	0.7149	0.9729	0.6858	0.9763	22.754
12_g	0.9450	0.7281	0.9645	0.6487	0.9752	20.713
13_g	0.9420	0.7338	0.9572	0.5559	0.9801	20.678
14_g	0.9226	0.7532	0.9354	0.4699	0.9803	20.284
15_g	0.9440	0.6894	0.9641	0.6029	0.9752	20.512
Average	0.9471	0.7326	0.9630	0.6027	0.9799	24.506
Standard deviation	0.0108	0.0290	0.0126	0.0634	0.0028	3.853
Maximum	0.9591	0.8007	0.9757	0.6858	0.9847	31.520

*Sensitivity (Se), Specificity (Sp), Positive Predictive Value (PPV), Negative PredictiveValue (NPV), Accuracy (Acc)

Table 4 shows comparison of performance of the proposed method with others published works. It can be observed that accuracy of the proposed method is comparable with others work on HRFID. In all categories: Healthy, DR, and Glaucoma, the proposed method scored the highest NPV compared to existing works. Furthermore, method by [18] time analysis is less than one minutes. [14] took 92 seconds and [19] less than 25 seconds whereas, the average time taken for the three types of image of the proposed method is 23.7402 seconds.

Table 4: Comparison of performance of the proposed method with others works.

Data set	Methods	*Se*	*Sp*	*PPV*	*NPV*	*Acc*
Healthy	Cheng et al. [18]	0.7889	0.9865	---	---	0.9647
	Annunziata et al. [19]	0.6820	0.9935	0.9271	0.9614	0.9587
	Odstrcilik et al. [14]	0.7861	0.9750	---	---	0.9539
	Proposed method	**0.7041**	**0.9771**	**0.7598**	**0.9699**	**0.9517**
DR	Cheng et al. [18]	0.6313	0.9851	---	---	0.9561
	Annunziata et al. [19]	0.6997	0.9787	0.7428	0.9729	0.9554
	Odstrcilik et al. [14]	0.7463	0.9619	---	---	0.9445
	Proposed method	**0.7390**	**0.9346**	**0.4927**	**0.9794**	**0.9206**
Glaucoma	Cheng et al. [18]	0.6921	0.9875	---	---	0.9634
	Annunziata et al. [19]	0.7566	0.9785	0.7567	0.9783	0.9603
	Odstrcilik et al. [14]	0.7900	0.9638	---	---	0.9497
	Proposed method	**0.7326**	**0.9630**	**0.6027**	**0.9799**	**0.9471**

*Sensitivity (Se), Specificity (Sp), Positive Predictive Value (PPV), Negative PredictiveValue (NPV), Accuracy (Acc)

5. Conclusion and Recommendations

In this paper, a new method for retinal blood vessel segmentation was successfully developed. The proposed method is categorized as unsupervised method. The proposed method was evaluated using HRFID dataset. Overall, the performance of the proposed method and comparable with existing works with overall accuracies were more than 90 % for all three different categories: healthy, DR and glaucoma. The method also required less time for execution. The proposed method had shown it effectiveness on unhealthy dataset thus it is believe that the method is meaningful when apply on real hypertensive retinopathy dataset. For future improvement of this study the following recommendations are suggested for the purpose of better performance of retinal blood vessel evaluation performance: i) construct the noise removal techniques to exclude lesion and ii) generalize the proposed method to other type of image database.

Acknowledgement

We thank the Pattern Recognition Lab (CS5), the Department of Ophthalmology, Friedrich-Alexander University Erlangen-Nuremberg (Germany), and the Brno University of Technology, Faculty of Electrical Engineering and Communication, Department of Biomedical Engineering, Brno (Czech Republic) for making the High-Resolution Fundus Image Database (HRFID) data available online. We would like also to acknowledge Universiti Malaysia Sarawak (UNIMAS). This work has been supported in part by Special Short Term Grant (SpSTG) MyRA F02/SpSTG/1374/16/16.

References

[1] Zhang J, Cui Y, Jiang W, Wang L, (2015), Blood vessel segmentation of retinal images based on neural network. In: *Image and Graphics*, ed: Springer, pp. 11-17.

[2] Wang S, Yin Y, Cao G, Wei B, Zheng Y, Yang G (2015), Hierarchical retinal blood vessel segmentation based on feature and ensemble learning. *Neurocomputing* 149, 708-717.

[3] Singh N, Kaur L (2015), A survey on blood vessel segmentation methods in retinal images. *International Conference on Electronic Design, Computer Networks & Automated Verification (EDCAV)*, pp. 23-28.

[4] Jiang K, Zhou Z, Geng X, Zhang X, Tang L, Wu H, *et al.* (2015), Isotropic undecimated wavelet transform fuzzy algorithm for retinal blood vessel segmentation. *Journal of Medical Imaging and Health Informatics* 5,1524-1527.

[5] Hassan G, El-Bendary N, Hassanien AE, Fahmy A, Snasel V (2015), Retinal blood vessel segmentation approach based on mathematical morphology. *Procedia Computer Science* 65, 612-622.

[6] Baker ML, Hand PJ, Wang JJ, Wong TY (2008), Retinal signs and stroke: Revisiting the link between the eye and brain. *Stroke* 39, 1371-1379.

[7] Chiang L-K, Yau MK, Kam C-W, Ng LV, Zee BC (2016), Epidemiological study of hypertensive retinopathy in the primary care setting: Retrospective cross-sectional review of retinal photographs. *Family Medicine and Community Health* 4, 13-21.

[8] Solkar SD, Das L (2017), Survey on retinal blood vessels segmentation techniques for detection of diabetic retinopathy. *Diabetes*.

[9] Stahl A, Hellström A, Smith LE (2016), Retinopathy of prematurity. In: *Anti-Angiogenic Therapy in Ophthalmology*, ed: Springer, pp. 21-29.

[10] Salazar-Gonzalez A, Kaba D, Li Y, Liu X (2014), Segmentation of the blood vessels and optic disk in retinal images. *IEEE Journal of Biomedical and Health Informatics* 18, 1874-1886.

[11] Kaba D, Wang C, Li Y, Salazar-Gonzalez A, Liu X, Serag A (2014), Retinal blood vessels extraction using probabilistic modelling. *Health Information Science and Systems* 2, p. 2, January 27 2014.

[12] Manikis GC, Sakkalis V, Zabulis X, Karamaounas P, Triantafyllou A, Douma S, *et al.* (2011), An image analysis framework for the early assessment of hypertensive retinopathy signs. *E-Health and Bioengineering Conference (EHB)*, pp. 1-6.

[13] Hassan H, Azis SFA (2012), A simple approach of blood vessels detection in retinal images using MATLAB. *IEEE Student Conference on Research and Development (SCOReD)*, pp. 245-249.

[14] Köhler T, Budai A, Kraus MF, Odstrčilik J, Michelson G, Hornegger J (2013), Automatic no-reference quality assessment for retinal fundus images using vessel segmentation. *Proceedings of the 26th IEEE International Symposium on Computer-Based Medical Systems*, pp. 95-100.

[15] Xu L, Luo S (2010), A novel method for blood vessel detection from retinal images. *BioMedical Engineering OnLine* 9, 14-14.

[16] Sridhar S, Rao S, Hemanth N, Nath MK (2015), An efficient blood vessel segmentation from color fundus image. *International Journal of Computer Applications* 119.

[17] Bahadar Khan K, Khaliq AA, Shahid M (2016), A morphological hessian based approach for retinal blood vessels segmentation and denoising using region based otsu thresholding. *PloS one* 11, p. e0158996.

[18] Cheng E, Du L, Wu Y, Zhu YJ, Megalooikonomou V, Ling H (2014), Discriminative vessel segmentation in retinal images by fusing context-aware hybrid features. *Machine Vision and Applications* 25, 1779-1792.

[19] Annunziata R, Garzelli A, Ballerini L, Mecocci A, Trucco E (2016), Leveraging multiscale hessian-based enhancement with a novel exudate inpainting technique for retinal vessel segmentation. *IEEE Journal of Biomedical and Health Informatics* 20, 1129-1138.